Environment Canada

Water Science and Technology Directorate

Direction générale des sciences et de la technologie, eau

Environnement Canada

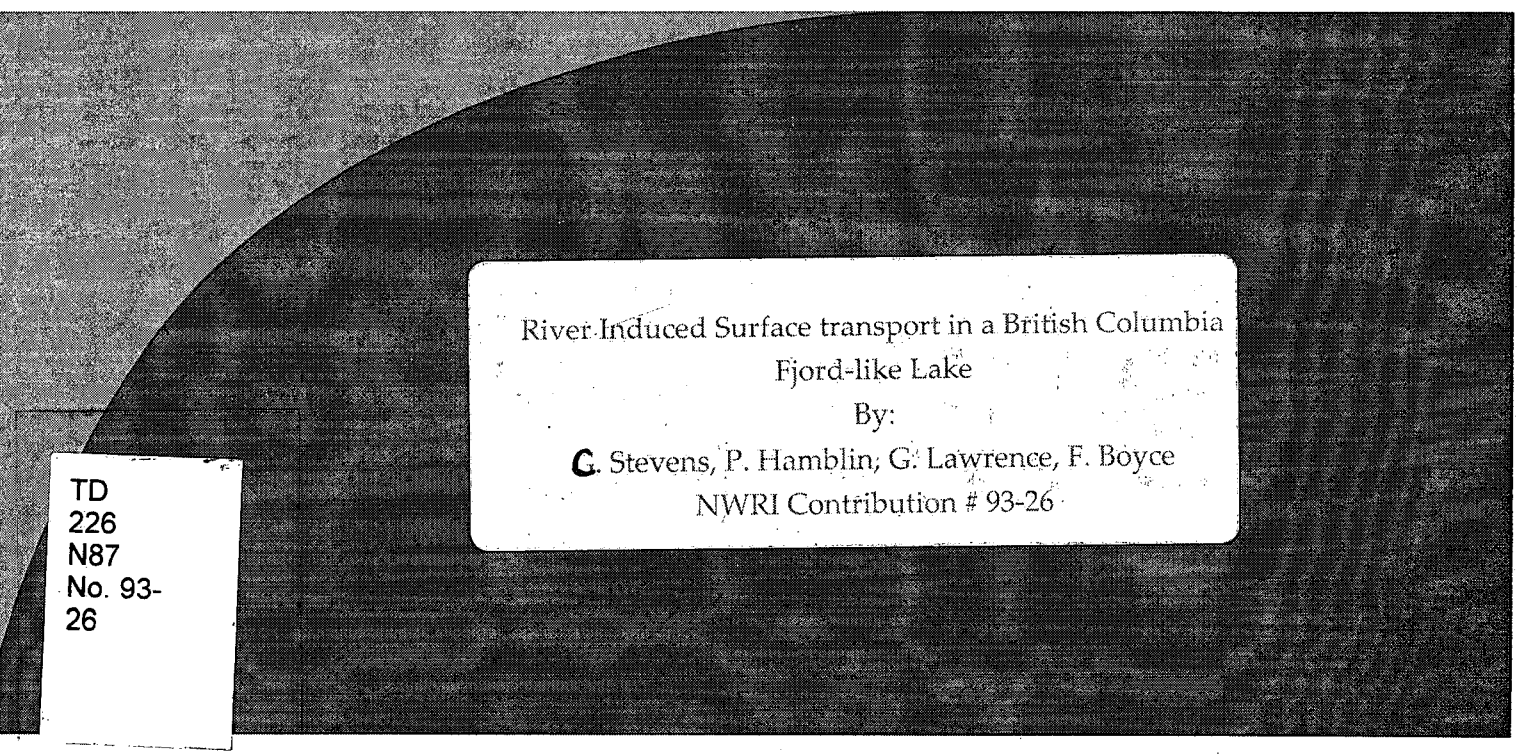

River-Induced Surface transport in a British Columbia Fjord-like Lake

By:

G. Stevens, P. Hamblin, G. Lawrence, F. Boyce

NWRI Contribution # 93-26

93-26

MANAGEMENT PERSECTIVE

Kootenay Lake, British Columbia's largest lake, has undergone dramatic shifts from over-enriched in the early 1970s to undernurished in the 1990s. Coincident with these water quality changes there has been a rapid decline in the economically important sports fishery; in particular, the Kookanee salmon and the Gerard rainbow trout. In response to the near critical level of these fish stocks a four-year program of artificial lake fertilization has been proposed by B.C. Environment.

As a component of this program strategies for most efficiently introducing the fertilizer were studied by the authors of this report. This paper concentrates on the evaluation of a proposal to use the natural river inflow to disperse the added nutrients. In another paper now in preparation by the same authors other methods are examined. Although this report was written at the University of British Columbia there is a strong contribution from NWRI. In this paper for the first time the eddy structure associated with river inflow into a fairly stagnant lake has been observed by NWRI's advanced acoustic instrumentation.

River Induced Surface Transport in a British Columbian Fjord-like Lake.

CRAIG L. STEVENS

Department of Civil Engineering, The University of British Columbia, B.C. V6T 1Z4

PAUL F. HAMBLIN

National Water Research Institute, Burlington, Ont., L7R 4A6

GREGORY A. LAWRENCE

Department of Civil Engineering, The University of British Columbia, B.C. V6T 1Z4

AND FARRELL M. BOYCE

National Water Research Institute, Burlington, Ont., L7R 4A6

STEVENS, C.L., P.F. HAMBLIN, G.A. LAWRENCE AND F. M. BOYCE, 1993 River induced surface transport in a British Columbian fjord-like lake. Can. J. Fish. Aquat. Sci.

Abstract

In response to a proposed Lake fertilization programme, a series of tracer experiments were carried out in the North Arm of Kootenay Lake in South Eastern British Columbia. Before this study the river inflow at the very Northern boundary of the lake was considered as a method of nutrient introduction and dispersal, herein we show that it is unpredictable and highly variable in its behaviour. Furthermore, the diurnal wind cycle dominates the mean circulation patterns and, as nutrients are taken up relatively quickly, it is the short term transport properties that are of interest here. Values of the apparent horizontal diffusion coefficient found in the river plume range over 2-15m^2s^{-1} and the overall dilution reaches typical values of 10^9 after several hours. This compares favourably with parametrized models for the diffusion coefficient.

1. Introduction

Artificial fertilization of lakes is occasionally considered as a solution to a range of limnological problems (Axler et al. 1988). In the spring of 1992, the British Columbia Ministry of the Environment commenced a fertilization program (Ashley and Thompson map 1993) in Kootenay Lake, the largest natural lake in British Columbia (Figure 1 a). It is hoped that the increased primary productivity of the lake will help to reverse the decline of Kokanee Salmon (*Onchorynchus nerka*) and Gerrard Rainbow Trout (*Onchorynchus mykiss*), although these declines have been attributed to a series of factors (Daley et al. 1981). The sensitivity of the natural environment and the substantial cost of introducing the nutrients (liquid ammonium polyphosphate and liquid ammonium nitrate) calls for an examination of (i) the effectiveness of the present nutrient injection method, (ii) the possibility that excessive build-up of nutrients might occur in some locations and (iii) possible options for improved distribution. To address these concerns we require a better understanding of the physical transport mechanisms active in the surface waters of Kootenay Lake, particularly at the northern end of the lake where the nutrients are injected. Thus, field experiments were carried out in late spring of 1992. The emphasis of this paper is on the role of the inflowing Duncan River at the north end of the lake in distributing the injected nutrients.

Figure 1b shows the general region of interest. The fertilization is planned for the North Arm of Kootenay Lake. The seasonal circulation pattern identified by Carmack et al. (1986) describes the lake structure as a deep, stagnant, hypolimnion topped by an active surface layer that forms after the winter overturn and increases in thickness to between 40-60 metres by the end of summer. The Kootenay and Duncan Rivers, in the South and North respectively, generate the bulk of the inflow to the lake. Water leaves the main lake via the shallow and narrow connection to the West Arm, and from there, via the Kootenay River to the Columbia River. The two major inflows and the outflow are dammed. The Duncan River inflow is modeled by Carmack et al. (1986) as entering the lake at the surface early in spring and then flowing out along the base of the thermocline later in the summer. This riverine flow forms the main interest of this paper because it is perceived as the most constant driving force in the North-Arm system, creating velocities of the order of 2 cms^{-1} well away from the river mouth, and it might be expected to carry nutrients over the full length of the North Arm if they were introduced either into the river upstream of the lake or close to the river mouth. A separate paper is in preparation

detailing observations of circulation and transport within the main body of the lake.

The behaviour of a river entering a lake and its subsequent development under similar circumstances have been modeled in detail by Hamblin and Carmack (1978) and (1980). However these authors considered only the steady state behaviour. While these models reasonably describe the flow field, they are of limited use here because we are considering uptake of phosphorus and nitrogen into the system for which the time-scales are known to range from a few minutes to a few hours (Lean et al. 1987). Short-term variations in concentration must therefore be considered even if the riverine flow may be taken as steady.

This paper reports a field experiment designed to reveal both small-scale and short-term features of the surface circulation and mixing that could affect the distribution and efficacy of the introduced nutrients.

2. Transport of an injected tracer by water movements: a guide to physical concepts and terminology.

Readers with a background in physical limnology or oceanography may skip this section.

2.1 Physical Principles

The concentration of dissolved nutrients at a fixed point in the lake changes with time as waters of differing nutrient concentrations move past the point and as nutrient concentrations are changed by the biological and chemical processes of uptake and/or regeneration (Boyce 1974). The usual mathematical form of the above statement is a differential equation that balances advection and diffusion and is called the equation of conservation of species,

$$\frac{\partial C}{\partial t} = S - (U.\nabla)C + \nabla(\kappa_c \nabla C), \qquad (1)$$ conserve

where U is the fluid velocity vector, the vector κ_c represents the apparent diffusivity of a tracer of concentration C in different directions, i.e. $\kappa_c = (\kappa_x, \kappa_y, \kappa_z)$, $\partial/\partial t$ is the partial derivative with respect to time, S is a source or loss term and ∇ is the gradient operator. Here we label the apparent diffusivity in the principal flow direction as κ_x and that in the normal direction as κ_y.

The left hand side of equation (1), $\partial C/\partial t$ is the time rate of change of nutrient (or tracer) concentration observed at the control point. There are three terms on the right hand side. The first represents the local rate of regeneration or removal. For the

purposes of this paper, sources include the fertilizer or dye injection and losses include decay due to the action of ultraviolet radiation for Rhodamine WT dye-tracer, and for the fertilizer, uptake by the local biomass. Adsorption to settling particles acts as a loss for both species. Our paper is not concerned with this term directly, but we cannot interpret the meaning of local changes in nutrient or tracer concentrations without knowledge of it. The last two terms portray the net water-borne flux of nutrient into an infinitesimally small control volume surrounding the point of interest. Our experiments seek to measure the last two terms.

If we were to measure the components of velocity and the nutrient concentration continuously with high resolution we would find a complex superposition of slowly varying, and rapidly varying fluctuations. The slower variations can usually be related to major energy inputs to the lake, such as wind, river flows, heating and cooling for water motions, nutrient (tracer) inputs and uptake. The more rapid fluctuations are seemingly random and are generally associated with the turbulent nature of large scale flows where viscous forces are too weak to transfer the organizing effects of flow boundaries to mid-channel. The distinction between the slowly varying "organized" fluctuations and "disorganized" turbulent fluctuations is imposed by the observer and reflects his or her particular interests. The effects of the organized fluctuations manifest themselves in the second term on the right hand side of (1) where the fluid flow moves parcels of water of different concentrations to the point of observation. Even if the details of the random turbulent fluctuations are not of interest, their global effect must nevertheless be accounted for because they may be the agents of significant fluxes of materials and momentum. A common way of treating these fluctuations in the context of equation (1) is to imagine the turbulent component of flow as consisting of finite eddies or blobs of fluid that exchange properties with each other in a manner analogous to diffusion processes operating at molecular scales.

The third term in equation (1) expresses the global effect of turbulence as a diffusion process where the flux of nutrient is proportional to the large scale "non-turbulent" concentration gradient. The constant of proportionality has the dimensions of diffusivity and, consequently, is called the eddy diffusivity. A virtue of this formulation is that its mathematical expression is identical to that of the flux of heat in a material of spatially varying thermal conductivity; a widely-explored problem of mathematical physics with results that can be transferred at least qualitatively. The principal difficulty with this

formulation is that there is no sufficiently understood way in which the eddy diffusivity can be defined in terms of easily measured flow parameters.

Equation (1) together with other equations that express the conservation of momentum (balance of forces) are readily approximated in finite difference form as the basis of mathematical models of lake behaviour (Walters et al. 1991) and many investigators have coupled physical, chemical and biological processes into "systems" models of complete lake behaviour, in which the lake is viewed as a stack of finite-sized compartments. The models excel at "keeping the books", that is to say, keeping track of the exchanges between the compartments as they are defined by the modeller, but ultimately their verisimilitude depends on parametrization of processes such as turbulent mixing, nutrient uptake, regeneration and energy transfers between trophic levels, in terms of the field variables of the model.

schematic

Figure 2 a illustrates two "snapshots" of a cloud of tracer injected into a stratified water column. Consider how this behaviour might be represented by a numerical (finite difference) equivalent of equation (1) applied to discretized model lake (Figure 2b) where the fluid is partitioned and each section assigned a concentration value. By stepping in time and accounting for the terms described in (1) it is possible to follow developments in the model concentration distribution. For both components of the mass transport, terms 2 and 3 on the right hand side of (1), the net flux of tracer into an element of the model depends on the difference in concentration of tracer between the element in question and the concentrations in all the surrounding elements. The advective term, term 2 on the right-hand side of (1) wherein the water velocity field is considered explicitly, is frequently the largest transport term. The velocity field is highly variable due to the cyclical nature of wind and river driven currents. The wind field has a diurnal cycle and the riverine outflow is partly controlled by the hydroelectric Duncan Dam release program which may vary by 40 percent of its maximum flow rate in one day. Furthermore the internal wave field imposes velocities in excess of 0.3 ms^{-1} and these waves have periods of many days and maximum amplitudes sometimes comparable to the depth of the lake (Wiegand and Carmack 1986) in exceptional circumstances.

The interaction of turbulence, stratification and velocity shear mean that it is almost impossible to prescribe a universal relationship for the apparent diffusivity κ_c in (1). Molecular rates of diffusion for the tracer are a lower bound for κ_c. An upper value for κ_c might be taken from the engineering literature for apparent diffusion in a bounded

turbulent flow with vertical shear (Fischer et al. 1979). However, as stratification provides some resistance to transport in the vertical direction, the appropriate values here lie somewhere in between. Csanady (1973) summarizes a quasi-empirical method developed by Okubo (1971) whereby the apparent horizontal diffusivity is related to the size of the cloud so that

$$\kappa_{x,y} = \alpha l^{\beta} \qquad (2)$$ okuboslaw

where α and β are empirically determined and l is the characteristic scale of the cloud. For isotropic turbulence $\beta = 4/3$, however, the directionality and shear generated by the riverine flow mean that the expansion of the dye patch is uneven. Fischer et al. (1979) and Csanady (1973) emphasize caveats in applying this result, especially near boundaries, inflows and at small scales. Nevertheless, Lawrence at al. (1993) show that it does appear to remain valid under some of these conditions and observe general values for the coefficients to be $\alpha \approx 2 \times 10^{-2}$ and $\beta = 1.1$. Note that the α constant is dimensional and has units of $m^{(2-\beta)}s^{-1}$.

The first step in improving upon this quasi-empirical model is to explicitly include the effects of shear dispersion (Csanady 1973 and Fischer et al. 1979). Shear dispersion occurs here when the river inflow or wind events create vertical or horizontal velocity gradients. While these gradients may appear to have minimal impact on (1), they do effect the apparent diffusivity of the water column by stretching out the tracer cloud as the background turbulence smears the cloud. The result is a diffusivity greater than that associated with the turbulence alone. The apparent horizontal diffusion coefficient that incorporates shear dispersion is a function of the eddy diffusivity in an equally turbulent, but unsheared, flow and the velocity shear.

Direct observations allow identification of the important terms and parametrization in equation (1), an essential step towards modelling the flow in an efficient and accurate manner. It is clear that the velocity-based parametrization of mass transport employed by Walters et al. (1991) to describe $\partial C/\partial t$ is incomplete and that we must include diffusive effects as well as advective motion. Furthermore, as Figure 2b makes very clear, the accuracy of the model depends very strongly on how the model compartments are chosen in relation to the observed spatial and temporal variability. There are two paths open, firstly a model might consider the diffusivity to be solely a function of the local small scale turbulence, and handle the large scale variations by having small grid sizes and time-steps. The second option is to use coarse grid spacing and time-steps and to attempt

to parametrize variations within the steps, a technique termed subgridscale modelling.

3. The Experiments: Location and Methods

3.1 Location

Kootenay Lake is a long (110 km), narrow (average width 3 km), deep (100 m), steep-sided fjord-like lake. It forms part of the Columbia River system and has its major inflows and outflow regulated by hydroelectric dams. The study examined only the northernmost region of the lake from Schroeder Point (Figure 1b). The very northern boundary of the lake is essentially the Duncan River delta, and is formed by a complex and changing satimg pattern of streams. Figure 3 shows sections from a SPOT satellite scene illustrating the convoluted flow paths taken by the Duncan River before entering the lake. The main river path in the delta is clearly visible, initially coming down the central axis of the lake and then sharply moving to the east and finally it enters the lake more or less running directly south. The river path changes rapidly over time-scales as short as a week.

The ongoing B.C. Ministry of the Environment's fertilization programme injects nutrients into the water column from a barge travelling down the centre of the lake between Lardeau Point and Schroeder Creek. Thus we selected sites at Lardeau, in the river plume near the village of Argenta, and at various sites south of Lardeau, away from direct influence of the river.

3.2 Moored, self-recording instruments.

Vertical arrays of self-recording thermographs and thermistors were installed in mid-lake at Lardeau, Lost Ledge Creek, Schroeder Creek and further south at the entrance to the West Arm. The arrays were sampled at one minute intervals and yielded a set of time series approximating the vertical temperature profile at each station throughout the experimental period. A meteorological recording system was deployed on a raft at the Lost Ledge mid-lake site, recording air temperature, humidity, vapour pressure, wind speed, wind direction, and incoming solar radiation every 10 minutes.

3.3 Measurements of Water Movements and Tracer Concentration.

Rhodamine WT dye was used as a tracer to delineate transport and mixing processes in the surface layer. Two launches were required for these measurements. The first carried a dye injection apparatus (pump and diffuser) and Rhodamine WT dye (specific gravity of 1.15 as supplied) premixed with methanol to near neutral density. This fluorescing dye is specifically designed for water/tracer experiments (Smart and Laidlaw

1977). The larger second vessel towed an instrument package that included a SeaBird Conductivity-Temperature-Depth (CTD) device and a Variosens fluorometer adjusted specifically for the Rhodamine WT. The instrument package could be made to undulate vertically through the top 50 m of the water column as the launch moved slowly ahead. A microwave positioning system provided horizontal control. All signals were sampled (0.67 Hz) and recorded digitally under the control of a microcomputer and the track of the launch was displayed graphically on the screen of a laptop computer. The spatial resolution of the measurements was typically around 1 m.

An Acoustic Doppler Current Profiler (ADCP) was mounted on a third launch through a well in the bottom of the hull. Its ultrasound signals beamed downwards and yielded estimates every 15s of water velocity relative to the boat at one meter intervals from 2 to 25m. In water less than 30m deep, the absolute velocity of the boat could be inferred from the bottom-reflected signal. At greater depths data from a satellite navigation system (Global Positioning System or GPS) were recorded with the ADCP data with a view to converting the relative ADCP information to absolute water velocities. The ADCP launch ran numerous "velocity" transects in the vicinity of the dye experiments. Unfortunately, a second GPS receiver intended to provide post-field differentially corrected GPS coordinates failed to operate. Consequently, only relative velocities can be inferred from the deep water measurements (greater than 30m). Nonetheless, the ADCP data are useful in providing vertical shear information in the vicinity of the dye to a resolution of 2-3 cms^{-1}. This is crucial for estimates of shear dispersion rates.

3.4 A typical experiment.

First the dye injection vessel deployed drogues in the area of the experiment for visual orientation and reference. Next, the dye (typically 40 litres of a methanol/Rhodamine WT mixture) was injected into the lake by pumping it through a flexible hose that terminated in a multi-port diffuser. The dye entered the water as a ring of small scale turbulent jets, thus ensuring significant initial dilution. The diffuser was lowered and raised repeatedly through the top 20 metres of the water column (approximately the photic zone) until the required amount was injected, a procedure that typically took 30 minutes. In the Duncan River, dye was poured in at the surface in a much shorter period (90 seconds in one experiment) because we could rely on river turbulence for initial dilution. The injections were made relatively quickly in order to reveal the short term flow variations that would have been obscured by a long slow release (e.g. Blanton and Ng 1971).

Before, during, and after the actual dye injection, the two other boats criss-crossed the study site with the ADCP and the CTD package. Thus, spatial and temporal observations of the dye were made while simultaneously recording the background physical properties of the water column.

4. Observations

Because Kootenay Lake lies in a steep-sided valley between the Purcell and Selkirk mountains, the winds blow mainly up and down the lake, approximately north and south. Southerly winds in this study period usually occurred during the afternoon, reversing wind late in the evening to generally weaker northerly winds. Figure 4 shows some of the meteorolgical data recorded at the Lost Ledge Creek site; the data includes wind speed and direction, solar radiation, vapour pressure and air and water temperature. The wind direction data illustrates a diurnal cycle that is broken only by the large wind event commencing on the evening of June 12th. The other data follows similar diurnal and synoptic trends.

The combined effect of the surface heating and cooling and the wind stirring resulted in a weakly but uniformly stratified water column, with changes of a few degrees over the top 20 m. The stratification varied with the passing of internal waves and the storm of June 12-13 fully mixed the top 25 m of the water column and created internal waves of amplitudes exceeding 10m.

4.1 River Plume Experiments

4.1.1 Experiment of June 12.

On June 12 1992, after dye was injected into the river several hundred metres upstream from the lake, the CTD and fluorometer package was held just beneath the surface at the main entrance to the lake. The resulting concentration-vs-time plot of Figure 5 dyedrograph shows that there was approximately a 25 minute delay before the dye appeared at the measurement site. In this experiment, unlike the usual rapid injections, the first 20 litres of tracer were introduced initially over twenty minutes and the last 20 litres over a period of over one hour. This two-phase injection manifests itself as a gaussian concentration curve followed by a substantial tail region as depicted in Figure 5. Such a tail is to be expected even with a rapid dye injection as the river obviously has back eddies and stagnant zones near the banks where some of the dye could accumulate and slowly leak back into the main flow.

The vessel tracks for the subsequent tracing of the dye plume are shown in Figure 6

shiptrack ; the path taken by the dye is apparent. Thanks to this real-time display, the instrument boat was able to track the dye rather than blindly swathing the expected area. The transect running NNE late in the day yielded a set of contours showing the structure of the dye plume. The natural log of the normalised dye concentration (relative to the

nstransect north-south transect background concentration, F_0) is shown in Figure 7 . It reflects the two-phase injection identified in Figure 5 and shows the riverine layer extending over the

tempprofile entire top 20 metres, the extent of the surface layer (Figure 8). The temperature-depth data recorded in the same area on the previous day identifies three distinct surface water temperatures, one associated with the riverine inflow and the other two further out into the lake. We observed debris lines near the river mouth that are associated with the riverine inflow plunging due to the warmer lake temperatures (maximum concentrations of dye were observed at 12 m depth). However, the significant entrance mixing and

adcpone convoluted flow patterns near the river mouth (Figure 9 a) mean that the dye is eventually distributed over the entire surface region. The ADCP data of Figure 9a identifies the velocity shear between the very surface water and the core region of the inflow (around 12 metres deep). This manifests itself with the appearance of a gravity current "nose" at depth as shown in Figure 7. Another feature from the ADCP data is the strong shear further to the west of the river plume, a consequence perhaps of entrainment into the plume or of the internal wave field at the time.

4.1.2 Experiment of June 17.

In a subsequent experiment on June 17 dye was injected into a different part of the river, a significantly colder inflow than that observed on June 12. The plume associated with this inflow manifested itself as a line of dye on the surface around the plunge line and concentrations at depths between 10 and 30 metres. It is noteworthy that the injections in the river delta, shown in Figure 3, on June 12 and June 17 took place only 100 m apart and yet their behaviour is totally different. The associated shear of the receiving water on June 17 is displayed in Figure 9b.

The mean velocity of the bulk of the plume on this day was around one third that of the June 12 experiment and typical dilutions were the order of 30 times smaller in this underflow than for comparable times with the surface flow.

4.2 Experiments away from the direct influence of the river flow.

Further south, away from direct influence of the river inflow, the wind is the major

driving force of water movements. It created long thin dye patches travelling downwind at substantial velocities (30 cm/s or, roughly, 1.2 km/hr) at the surface and almost stagnant conditions beneath the wind-driven region. In several instances these plumes evolved over a few hours so that they were several kilometres long and only two hundred metres wide. In one experiment the action of wind and the riverine flow appear to have combined. The plume spread out transversely to the direction of the wind and moved at a substantial velocity against the wind. This was observed in an experiment off Lardeau several kilometres away from the river mouth.

The experiment of June 14, the day following the cessation of the large storm than ran from June 12 through to late in the day of June 13, took place under light wind conditions, yet the advection of the plume and the subsequent dispersion were amongst the most complex experienced over the whole period. This is attributed to large scale internal waves and the effect of the Schroeder Creek headland. A day later, on June 15, an experiment near the shore at Lost Ledge Creek showed that the advection of the plume on this quiescent day was almost zero and minimum dilutions were smaller than for any other experiment. These open-lake experiments are the basis of a separate paper.

5. Discussion

The river inflow region is more hydrodynamically complex than we initially thought. We encountered at least two completely different waters entering the lake (Fig. 8) and sharing some of the network of channels in the delta region. We can expect therefore highly variable conditions that may depend on dam release schedules. During the late-spring conditions that we encountered the entrance mixing is vigorous. For example, tracer originally in the river water that has a depth of neutral buoyancy in the lake of around 10 metres, appears at the lake surface for almost all of the plume region (Figure 6). These conditions are not expected to last throughout the summer as the lake surface gradually warms while the inflow remains cool (depending on the strategy of release from the Duncan reservoir). A simple figure of merit for parametrizing the mixing associated with the inflow is the densimetric Froude number, Fr:

$$Fr^2 = \frac{u^2}{dg'}, \qquad (3)$$ froude

where d and u are the inflow thickness, which is the full depth, and velocity respectively, and g' is the reduced gravitational acceleration (Chu and Jirka 1987). This reduced gravity represents the buoyancy effect (density contrast between lake and river) such that

$g' = (\Delta\rho/\rho_0)g$ where $\Delta\rho$ is the density difference between the incoming water and the lake water of density ρ_0 and g is the gravitational acceleration. Roughly speaking, the scaling of the Fr suggests that a value much greater than approximately unity indicates that inertia associated with the inflow will overcome the stability provided by buoyancy and mixing will ensue. Conversely, if Fr is much less than 1 then the scaling indicates a stable non-mixing flow where turbulence is suppressed by buoyancy forces.

For the late spring conditions that we encountered, we estimate ($h = 20$m, $u = 0.1\text{ms}^{-1}$, $g' = 0.001\text{ms}^{-2}$, from Figures 8 and 9) that $Fr = 0.7$, indicating that the river plume mixes somewhat with the ambient lake water on contact. Taking values typical of late summer conditions ($h = 20$m, $u = 0.1\text{ms}^{-1}$, $g' = 0.01\text{ms}^{-2}$) Fr becomes 0.2 and we predict that the river plume is likely to remain a coherent flow at its depth of neutral buoyancy.

From observations of absolute velocities in the delta region it is apparent that stag-
adcptwo nant zones (i.e. Figure 10), regions where injected fertilizer might remain at high concentrations, occur frequently. Periodic pulsing of the reservoir release might help to flush such zones. Once the fertilizer has reached the open lake, however, it is unlikely to remain excessively concentrated because the ADCP data shows that the flow in the Lardeau region is active and variable; indeed we observed one example of a gyre shed by the Lardeau headland. In the main body of the lake the major driving force is the wind with its pronounced diurnal cycle. Anecdotal information received from local towboat operators suggest that gyres in the wind-driven circulation are formed in the lee of headlands such as Schroeder Point. So rather than the picture of a surface layer being slowly advected downwind as a homogeneous unit, the situation might be conceptualized as follows: the riverine flow near or at the base of the thermocline flows south along the North Arm of the lake at velocities of the order of 0.01 ms^{-1} while the surface water is being pushed up and down the lake at ten times that speed and also the headlands create strong cross-lake flows. From time to time, strong winds entrain the thermocline region into the surface layer, effectively distributing the river-input fluid. Systems models such as those developed by Walters and his co-workers to synthesize the lake fertilization program, may well operate at seasonal timescales, but must nevertheless incorporate parametrization of mixing that represent the vigour and complexity we have encountered, especially given likely uptake times.

By considering maximum dye concentrations found at various distances from the

river injection site it is possible to assemble a picture of the dye-cloud growth at various
dyeshape times (for example, June 12, Figure 11). The cloud changes from an initially highly concentrated peak to a relatively symmetric cloud to a flatter, lopsided distribution. Figure 11 can be viewed as a series of longitudinal sections through the main body of the plume as it moves southwards at an assumed constant velocity of 0.38 km/hr. This was estimated by consideration of the velocity of the apparent centre of mass of the dye cloud and also from the ADCP data. The effect of mean advection has been removed but not that of velocity shear in the water column nor that of variation of the mean velocity in time or space. Calculation of the standard deviation of this estimated dye patch (a standard technique in which the dye concentration is viewed as the probability distribution of a cloud of dye particles and the standard deviation becomes the root-mean-squared distance of a dye particle from the centre of the cloud, see Fischer et al. 1979) shows that it grows from just over 100 metres to nearly 600 metres. From Csanady (1973) it is possible to model the relative horizontal diffusion as

$$\kappa_{x,y} = \frac{1}{2}\frac{\sigma^2}{\Delta t}, \qquad (4)$$ sdeveqn

where σ is the standard deviation of the dye cloud and Δt is the time after introduction. Values of κ_x found in this way from Figure 11 range from 2 to almost $15 \mathrm{m}^2\mathrm{s}^{-1}$. However, if we now look at the distribution of dye normal to the main flow, a different picture
ewtransect emerges. Figure 12 shows that the plume here is only a few hundred metres wide. The dispersion normal to the flow is significantly weaker than in the direction of the flow. The standard deviations are between 100m and 300m and diffusion coefficients are all less than $5\ \mathrm{m}^2\mathrm{s}^{-1}$.

If we first use the model described by (2) we find a value for the horizontal apparent diffusivity using (2) to be $\kappa_{x,y} \approx 19 \mathrm{m}^2\mathrm{s}^{-1}$ for, $l = 500$, the horizontal characteristic lengthscale of the patch size, which is taken here to be the diameter of the patch if it were radially symettric. This is only marginally greater than our observations. Further pursuing this case, the value of the horizontal apparent diffusivity measured above may be compared to the theoretical value for the apparent horizontal diffusivity including shear dispersion, (Fischer et al. 1979) in a vertically bounded two-dimensional uniform shear flow,

$$\kappa_x = (du/dz)^2 H^4/(120\kappa_z) \qquad (5)$$ sheardispersion

where the observed shear, du/dz, is $5. \times 10^{-3} s^{-1}$ from the ADCP plots of Fig. 9a, the

depth over the shear layer is $H = 10$m, and the vertical eddy diffusivity κ_z, is a function of surface wind stirring and the near-surface stratification.

Based on the recent mixing efficiency measurements in lakes by Imberger and Ivey (1991) we estimated the vertical unsheared turbulent eddy diffusivity to be approximately one hundred times greater than molecular diffusion of momentum (i.e. $\kappa_z = 10^{-4}$ m^{2}s^{-1}). Thus, κ_x is estimated to be 21 m^{2}s^{-1} which again compares favourably with the observations. A possible explanation for our observations being lower than this estimate is that the assumption that the density interface at the base of the riverine flow does not act exactly like the solid boundary used to formulate (5). Instead, entrainment as described by (3) causes the boundary to deepen.

Conclusions

Recall that the objective of the study was to identify transport behaviour and from that understanding, (i) quantify the effectiveness of the present nutrient injection, (ii) identify regions of excessive buildup and (iii) suggest options for improved introduction of fertilizer. The emphasis here being on the importance of the riverine flow.

The first objective can be crudely met by considering the maximum dilutions of the injected dye as a function of time. As the fertilizer is injected into the propeller wash of the barge it is likely to be sufficiently mixed to behave in the same way as the neutrally buoyant dye (the raw fertilizer has a specific gravity of around 1.1). Table 1 shows typical values for the experiments, and as an extreme example, the highest concentration of dye found after significant mixing time occurred on a calm, warm day very near the shore at Lost Ledge Creek. In this experiment, concentrations exceeding $ln(F/F_0) = 6.5$ (a dilution of almost 10 million) remained very near the point of injection after 8 hours. The expected seasonally averaged riverine flow did not appear to have any obvious impact this close to shore. In most of the other experiments the maximum concentrations dropped below $ln(F/F_0) = 3$ (a dilution of more than 100 million) within 4 hours. Thus, assuming that biological uptake is not a limiting factor, the present method of fertilizer dispersal is quite effective. The material is introduced over a 10 km stretch of open water in a day. This distance is comparable to the maximum surface drift one could expect from a substantial wind event and much longer than the corresponding riverine drift. Furthermore, the initial dilution of the fertilizer at the point of injection will be augmented by a factor of at least 100 in the first 4 hours. It is more than likely that the

Table 1 here

wind field will reverse within 12 hours of the injection, further increasing the dilution of the fertilizer, but not necessarily displacing it along the lake any great distance. ADCP observations indicate that it will be adequately distributed in the across lake direction near any of the headlands. Thus, any shore-based injection set-up should not be confined to one point along the North Arm with the expectation of having significant impact over the entire North Arm. Several injection sites would be required, preferably on the obvious promontories and in the river mouth. Introducing the fertilizer via the Duncan River, an option that has been proposed, is not recommended because it is unpredictable and high concentrations are likely to form in the delta region. It would prove to be a suitable injection vehicle if the injection could take place offshore away from the delta as part of the several injection sites mentioned above.

Acknowledgments

This work would not have been possible without the efforts of Ken Ashley, Carl Walters, Al Martin and Harvey Andrusak which led to funding from the B.C. Ministry of the Environment and B.C. Hydro. Funding was also supplied by NSERC. The field team included Noboru Yonemitsu, Chris Rogers, Leslie Gomm, Bernard Laval, Barry Moore, Charlie Talbot, Jim Diaz and Les Fleck. Mike Kory at Seaconsult and Eddy Carmack, David Topham and Dean Addison at IOS provided additional support. Cheng He's preparation of the ADCP data is gratefully acknowledged.

References

ASHLEY, K.I. AND L. THOMPSON, 1993 Kootenay Lake Fertilization Experiment Year 1 Report. Fisheries Project Report No. RD 32, British Columbia Ministry of the Environment, 55p.

AXLER R., L. PAULSON, P. VAUX, P. SOLLBERGER AND D.H. BAEPLER, 1988 Fish aid- the Lake Mead fertilization project. Lake and Reservoir Management 4(2), 125-135.

BLANTON, J.O. AND H.Y.F. NG, 1971 The circulation of the effluent from the Okanagan River as it enters Lake Skaha. internal report, Can. Centre Inland Waters, 25p.

BOYCE F.M., 1974 Some aspects of Great Lakes Physics of importance to biological and chemical processes. J. Fisheries Research Board of Canada 31(5), 689-730.

CARMACK, E.C., R.C. WIEGAND, R.J. DALEY, C.B. GRAY, S. JASPER AND C. H.

PHARO, 1986 Mechanisms influencing the circulation and distribution of water mass in a medium residence-time lake. Limnol. Oceanogr., 31(2), 249-265.

CHU, V.H. AND G.H. JIRKA, 1987 Surface buoyant jets and plumes. In Encyclopedia of Fluid Mechanics, ed. N.P. Cheremisinoff, Vol 6:1053-1084.

CSANADY G.T., 1973 Turbulent diffusion in the environment. Geophysics and Astrophysics Monographs, Vol. 3, D. Reidel, Dordrecht, pp..

DALEY, R.J., E.C. CARMACK, C.B.J. GRAY, C. H. PHARO, S. JASPER AND R.C. WIEGAND, 1981 The effects of upstream impoundments on the limnology of Kootenay Lake, B.C.. Environment Canada, Scientific series no. 117, 98p.

FISCHER, H.B, E.J. LIST, R.Y.C.KOH, J. IMBERGER AND N.H. BROOKS, 1979 Mixing in Inland and Coastal Waters. Academic, 483p.

HAMBLIN, P. AND E. CARMACK, 1978 River induced currents in a fjord lake. J. Geophys. Res., 83, 885-899.

HAMBLIN, P. AND E. CARMACK, 1980 A model of the mean field distribution of a dissolved substance within the riverine layer of a fjord lake. Water Resources Res., 16, 1094-1098.

IMBERGER, J. AND G.N. IVEY, 1991 On the nature of turbulence in a stratified fluid, part II: application to lakes. J. Phys. Oceanogr. 21, 659-680.

LAWRENCE, G.A., K.I. ASHLEY, N. YONEMITSU AND J.R. ELLIS, 1993 Natural dispersion and the fertilization of a small lake. unpublished manuscript, contact authors.

LEAN D.R.S., A.A. ABBOTT AND F.R. PICK, 1987 Phosphorus deficiency of Lake Ontario plankton. Can J. Fish Aquat. Sci. 44, 2069 - 2086.

OKUBO, A., 1971 Oceanic diffusion diagrams. Deep-Sea Research, 18, 789-802.

SMART, P.L. AND I.M.S. LAIDLAW, 1977 An evaluation of some fluorescent dyes for water tracing. Water Resources Res., 13, 15-33.

WALTERS, C.J., J. DIGISI, J. POST, J. SAWADA, 1991 Kootenay Lake fertilization response model. Fisheries Management Report No. 98, 36p.

WIEGAND, R.C. AND E.C. CARMACK, 1986 The climatology of internal waves in a deep temperate lake. J.Geophys.Res., 91(C3), 3951-3958.

Measurement	F (ppb)	$\ln(\frac{F}{F_0})$	dilution
raw mix	10^9	22	1
initial	3600	9.6	3×10^5
spike	100	6.0	10^7
dye cloud	1	1.5	10^9
background	0.23	0.0	4×10^9

Table 1; Tabulated list of typical concentrations, F is the dye concentration in parts per billion (ppb) and F_0 is the background level of fluorescence which typically manifested itself as 0.23 ppb.

Figures

Figure 1. (mainmap) Shoreline data for (a) the entire main lake and (b) the study site at the Northern end of the North Arm. The triangles indicate positions of the main thermograph arrays and the meteorological data was recorded at the array location adjacent Lost Ledge Creek.

Figure 2. (schematic) A schematic illustration of (a) what happens to some tracer when acted upon by a sheared, stratified environment and (b) how this might then be discretized. Each box in (b) represents a concentration that must use an approximation of (1) to estimate how it changes in time.

Figure 3. (satimg) SPOT satellite data with resolution of 5 x 5 metre pixels, showing the Duncan River delta. The main flow path is obvious, however indicators of several secondary flow paths are also apparent.

Figure 4. (wind) A multi-panel figure showing meteorological data including (a) wind direction where 0 degrees represents a wind from the North, (b) wind speed, (c) solar radiation, (d) vapour pressure and (e) air and surface water temperatures.

Figure 5. (dyedrograph) The data recorded on June 12th 1992 at the Duncan River main entrance into the lake. Also included is the best-fit gaussian distribution to the initial portion of the curve.

Figure 6. (shiptrack) Shiptracks for June 12 1992.

Figure 7. (nstransect) A contour plot of $ln(F/F_0)$ where F is the observed dye concentration and F_0 is the background reading in the lake surface water. The transect is on a line running up the middle of the dye cloud from the South. The actual locations that

data were recorded is shown as dots on the plot.

Figure 8. (tempprofile) Temperature plotted against depth for June 11.

Figure 9. (adcpone) Vectors representing vertical shear of horizontal velocity where the velocity is averaged over the depths 16 to 20m and 21 to 25 m, in the water column on (a) June 12 and (b) June 17, 1992.

Figure 10. (adcptwo) Vectors representing absolute horizontal velocity on June 17, 1992, averaged vertically over (a) 1-4m, (b) 5-8m, and (c) 9-12m.

Figure 11. (dyeshape) Dye distributions along the north-south axis of the dye cloud at several times on June 12 1992.

Figure 12. (ew transect) Similar to Figure 7 but instead based on an east-west transect for June 12, 1992.

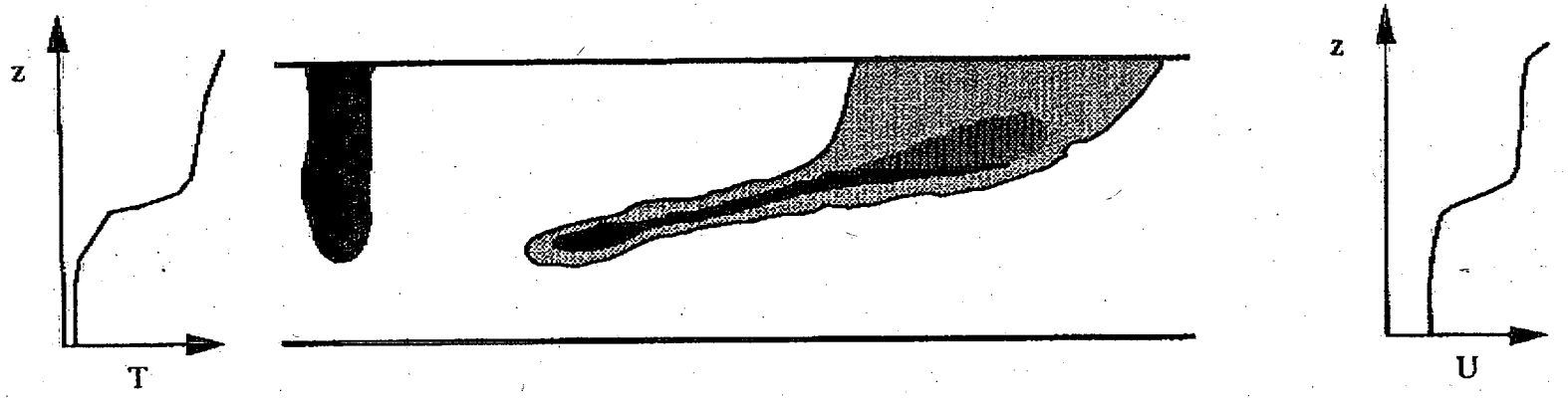

(a)

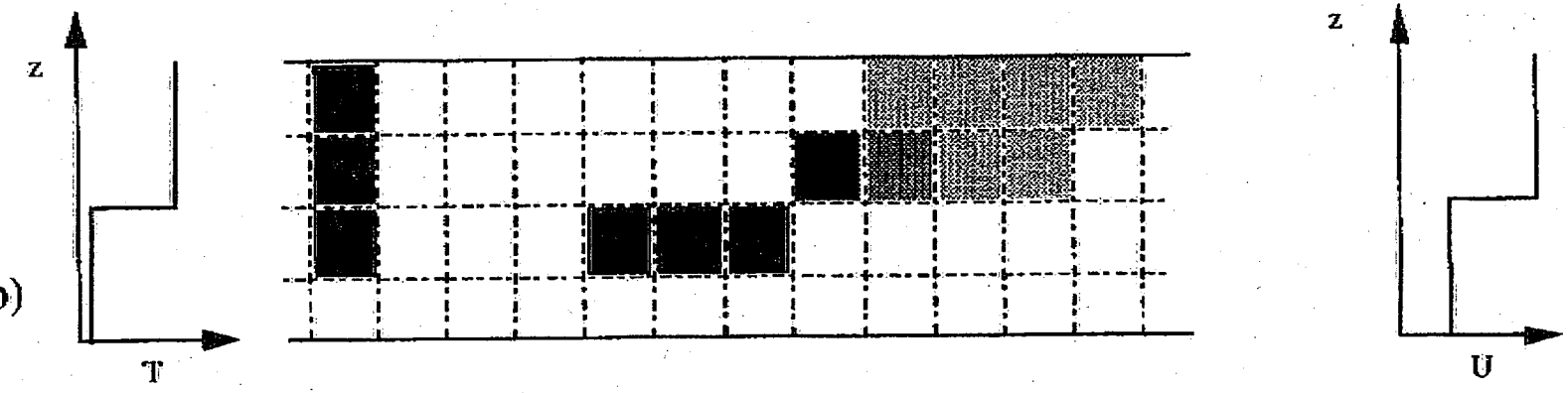

(b)

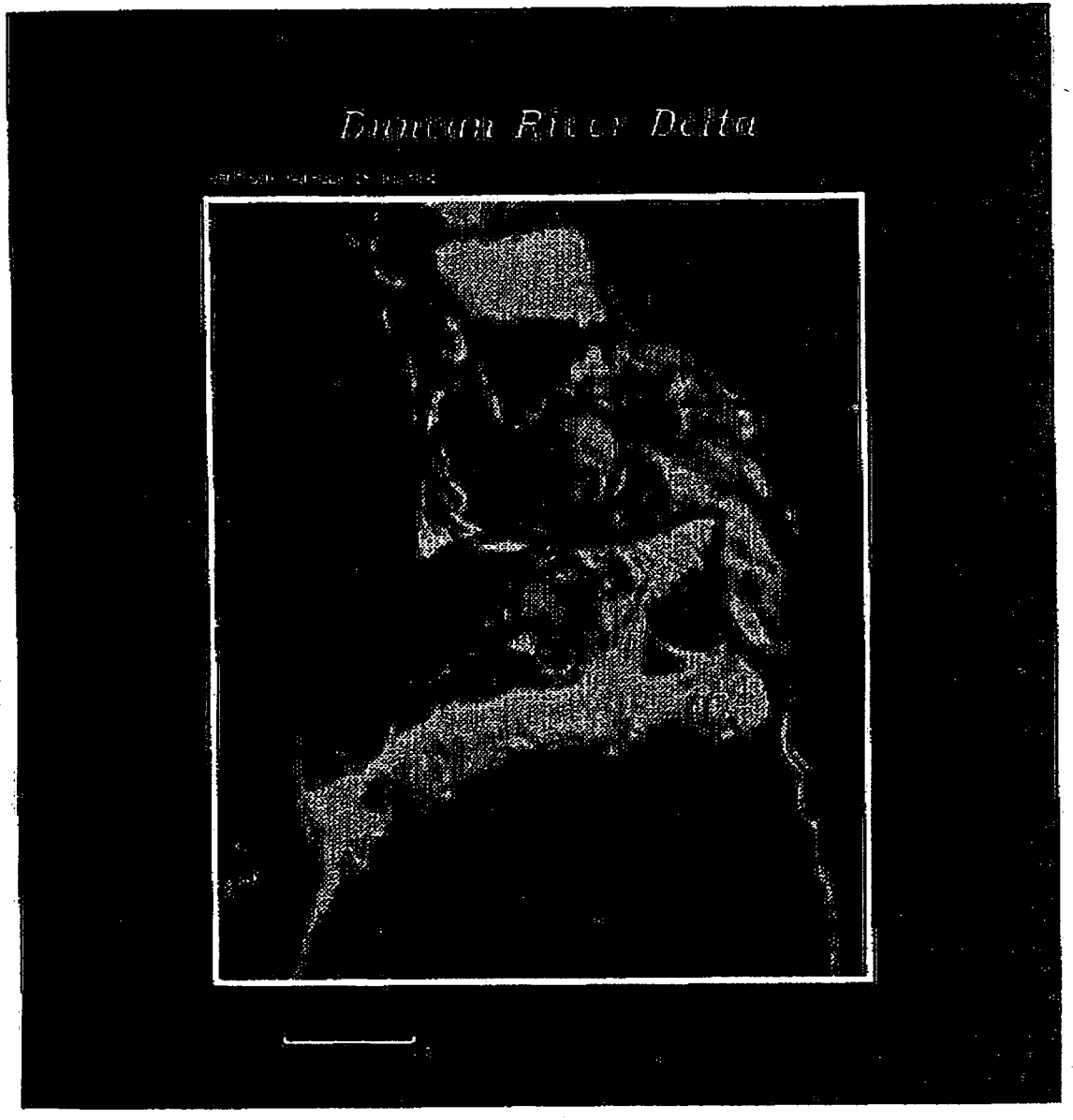
Duncan River Delta

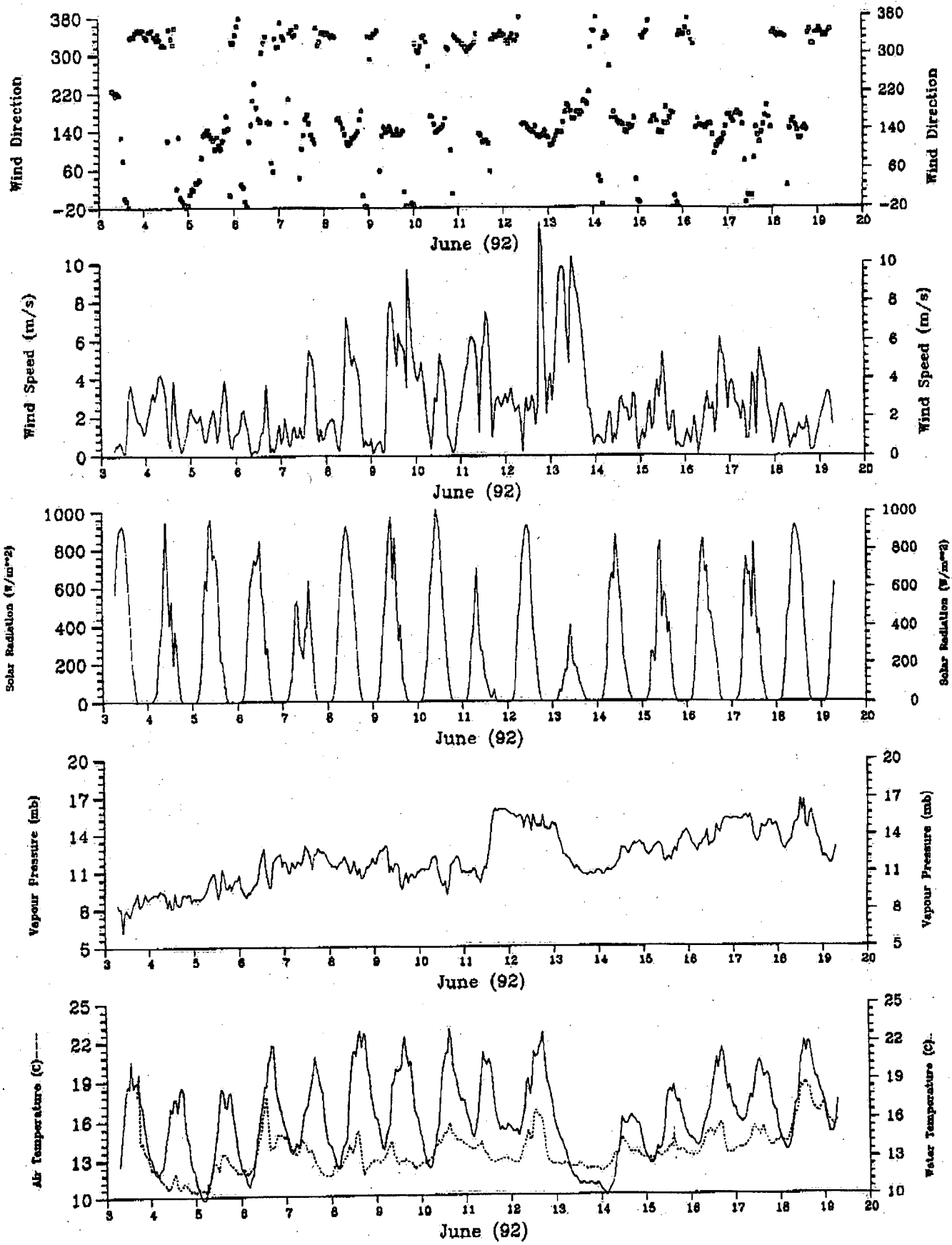
Wind Direction
380
300
220
140
60
-20
3 4 5 6 7 8 9 10 11 12 13 14 15 16 17 18 19 20
June (92)
Wind Speed (m/s)
10
8
6
4
2
0
June (92)
Solar Radiation (W/m**2)
1000
800
600
400
200
0
June (92)
Vapour Pressure (mb)
20
17
14
11
8
5
June (92)
Air Temperature (C)
Water Temperature (C)
25
22
19
16
13
10
June (92)

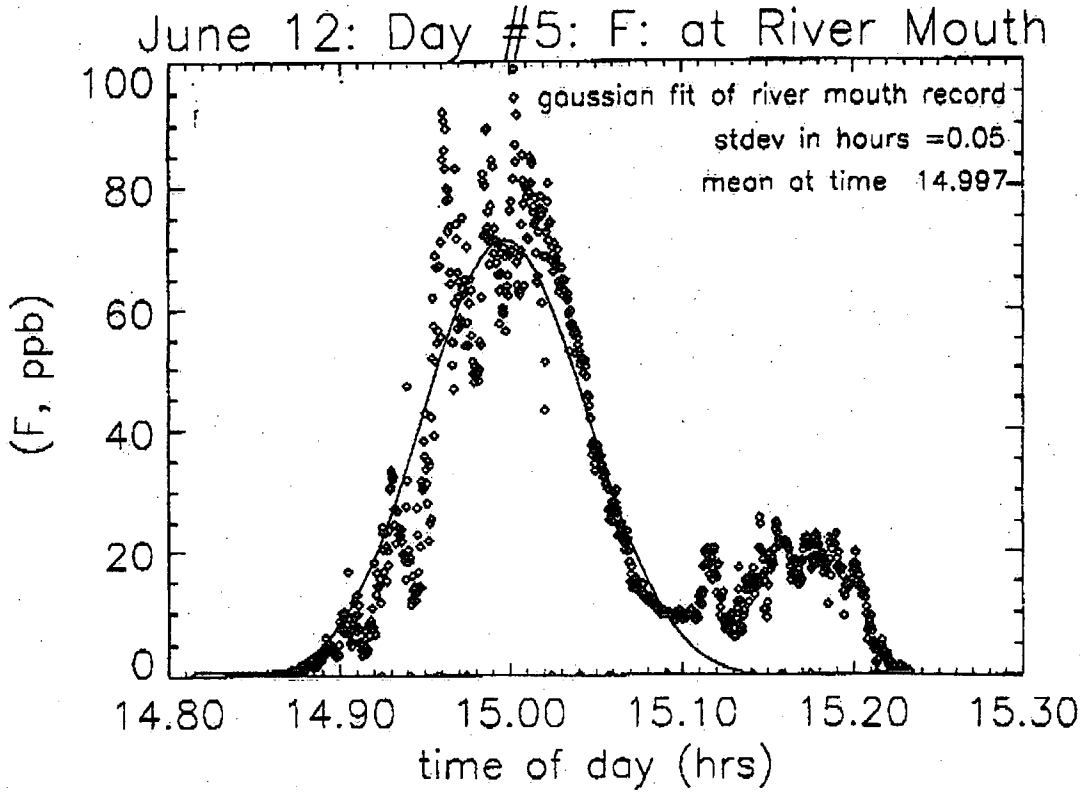
June 12: Day #5: F: at River Mouth
gaussian fit of river mouth record
stdev in hours =0.05
mean at time 14.997
(F, ppb)
100
80
60
40
20
0
14.80
14.90
15.00
15.10
15.20
15.30
time of day (hrs)

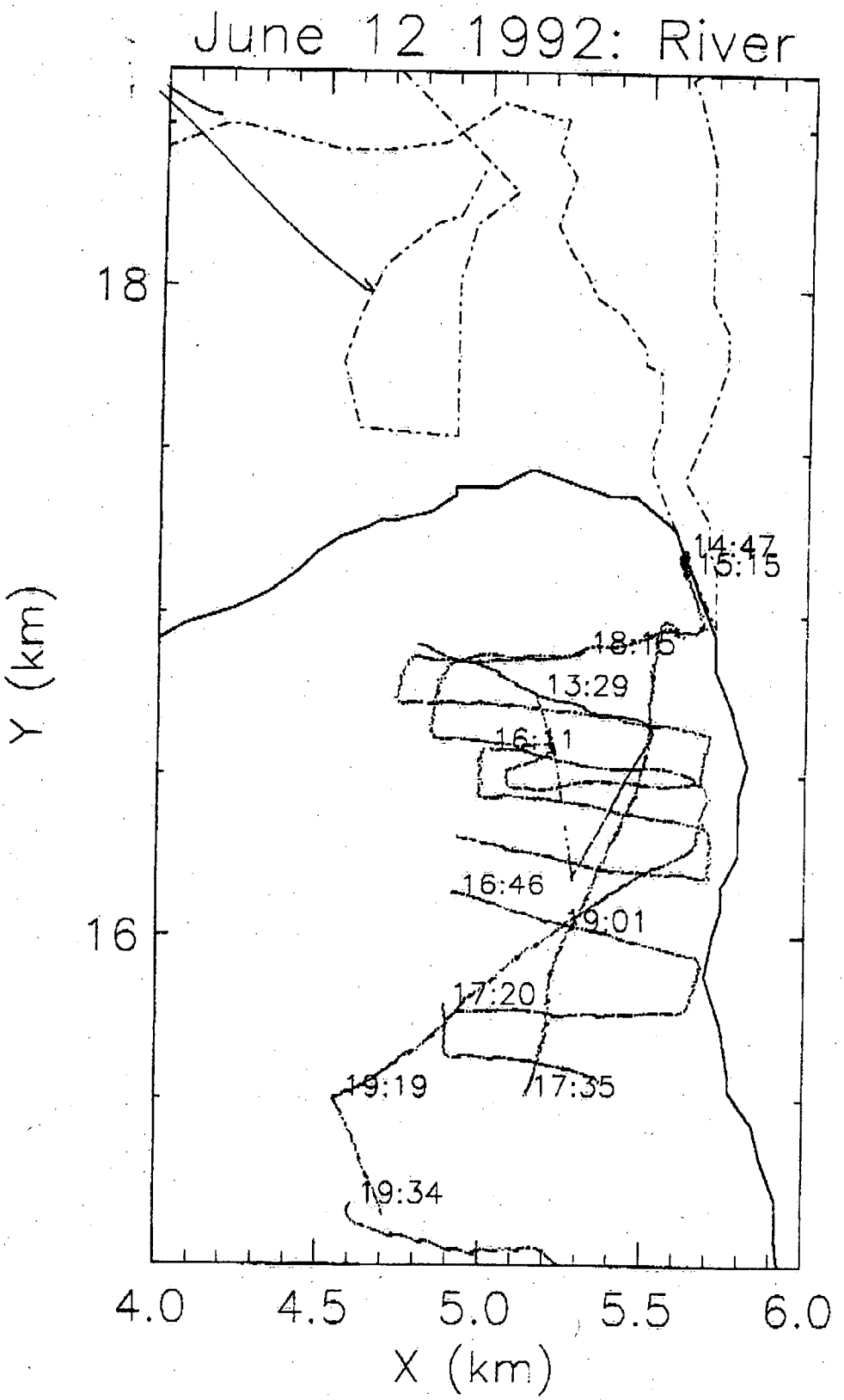
June 12 1992: River
18
16
Y (km)
14:47
15:15
18:15
13:29
16:11
16:46
19:01
17:20
19:19
17:35
19:34
4.0
4.5
5.0
5.5
6.0
X (km)

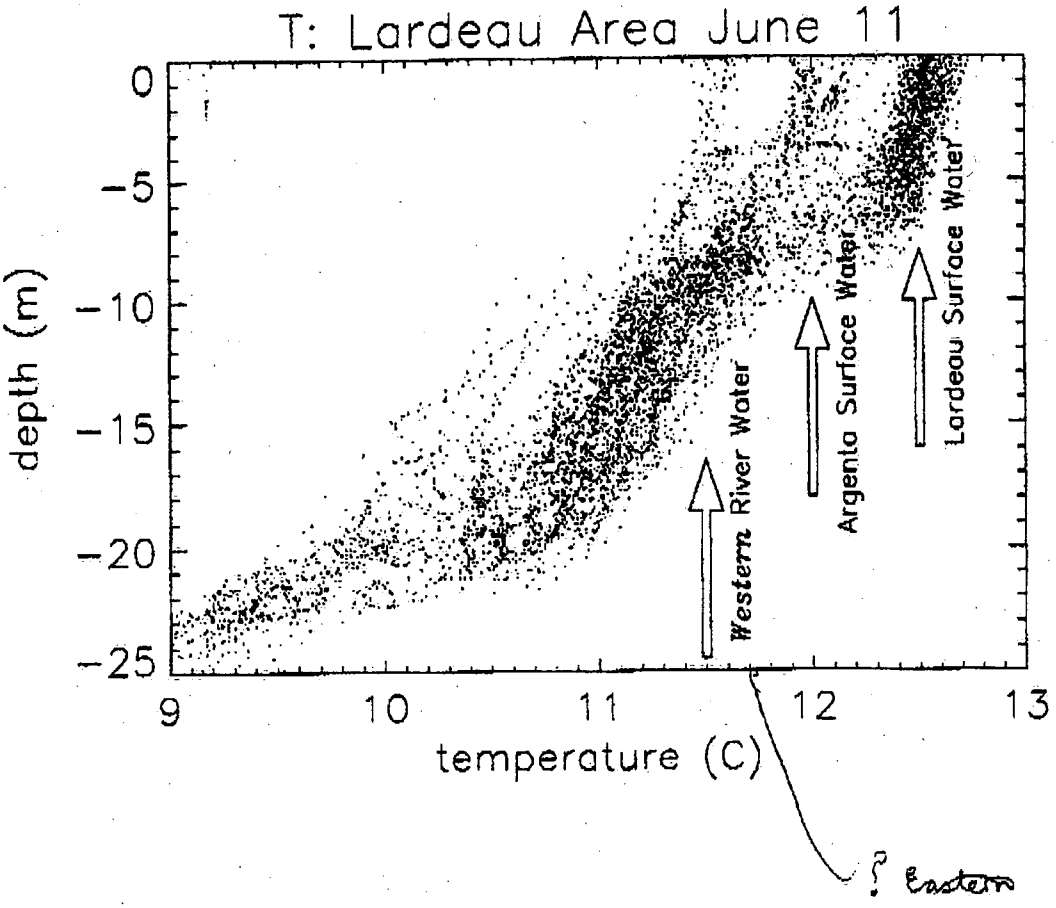
T: Lardeau Area June 11
depth (m)
0
-5
-10
-15
-20
-25
9
10
11
12
13
temperature (C)
Western River Water
Argenta Surface Water
Lardeau Surface Water
? Eastern

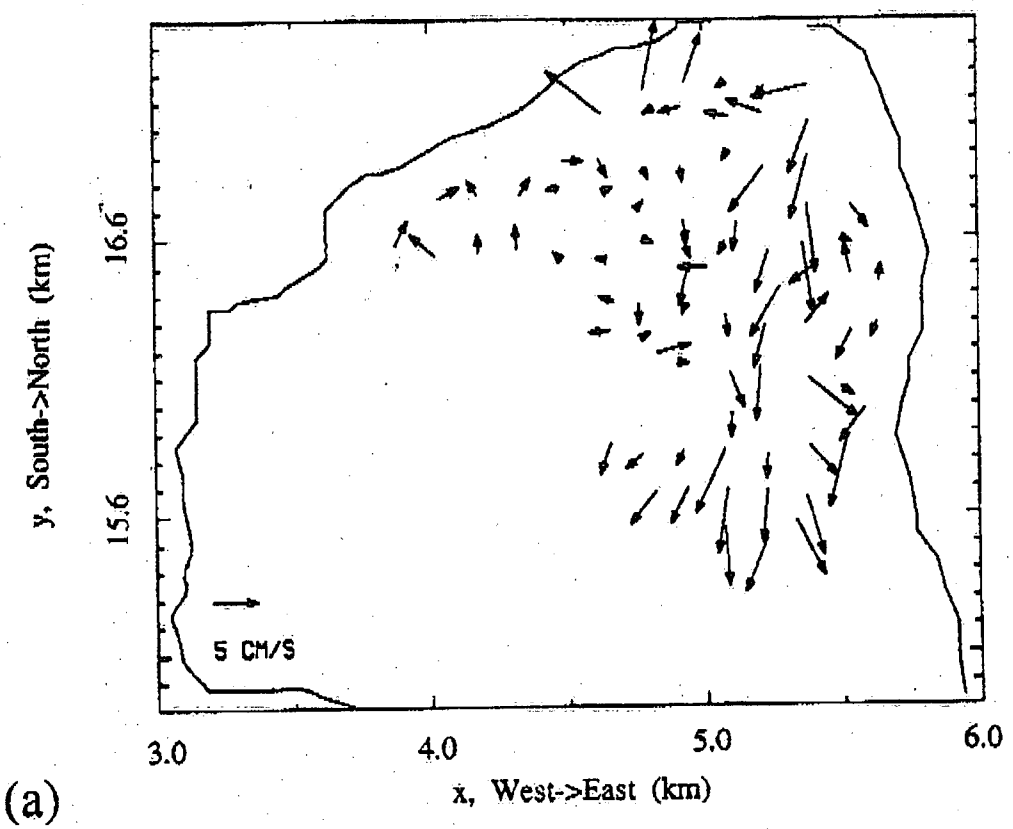
y, South->North (km)
16.6
15.6
5 CM/S
3.0
4.0
5.0
6.0
x, West->East (km)

(a)

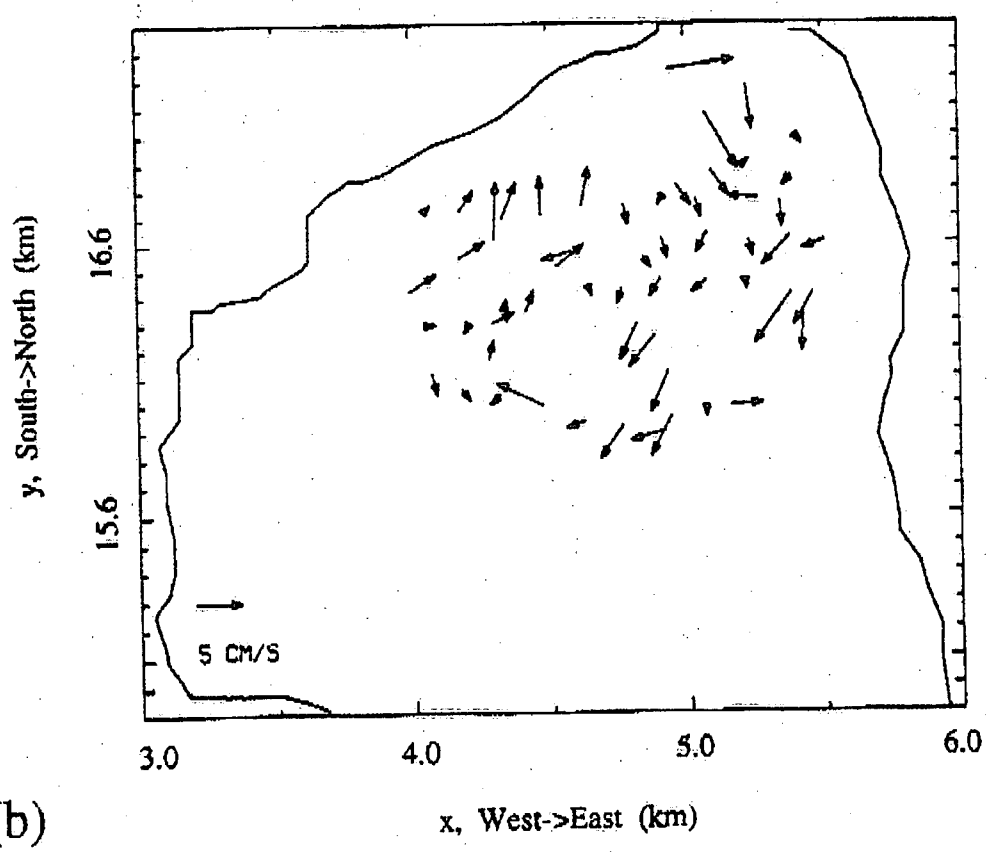
y, South->North (km)
16.6
15.6
5 CM/S
3.0
4.0
5.0
6.0
x, West->East (km)

(b)

fig 9

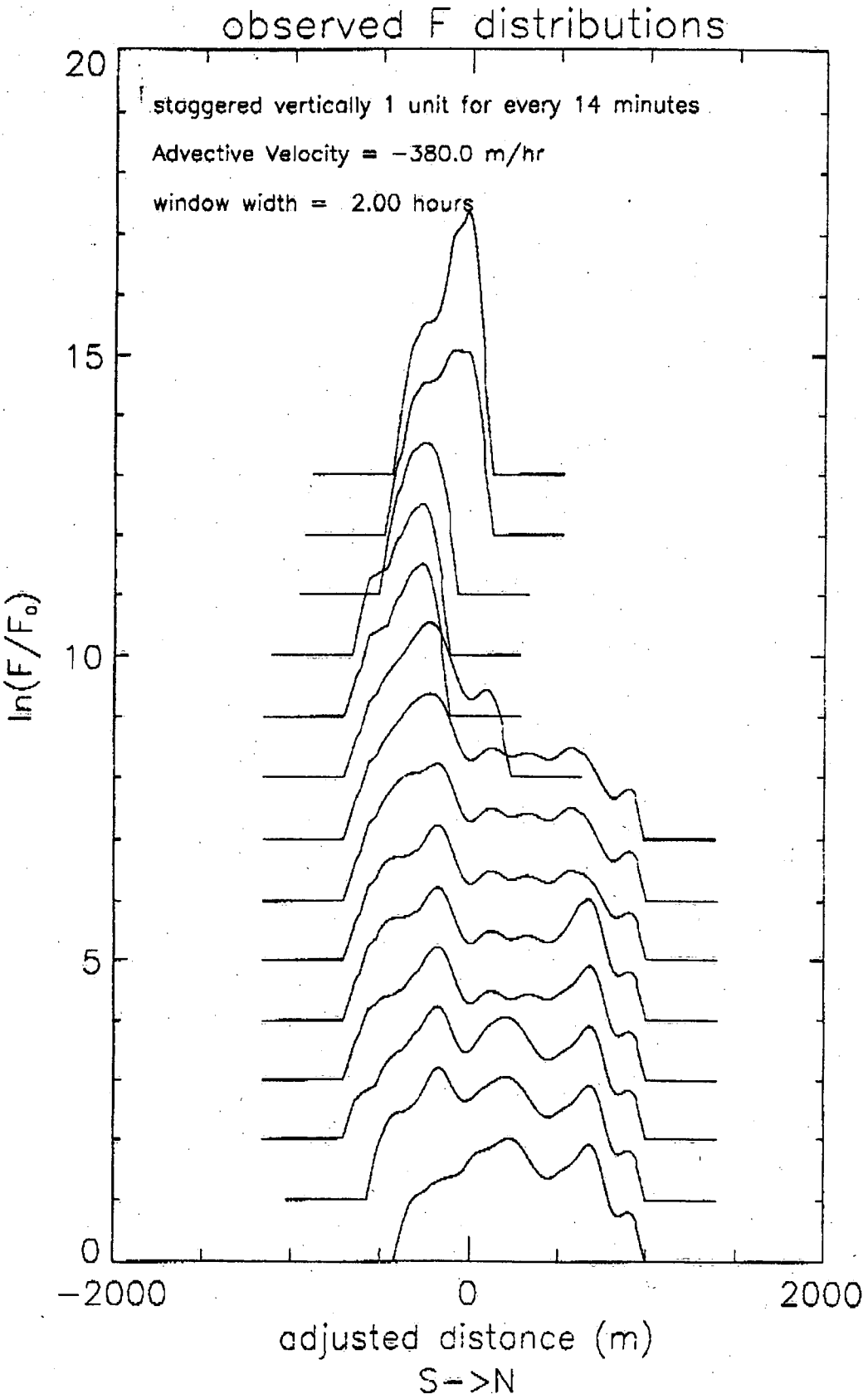
observed F distributions
staggered vertically 1 unit for every 14 minutes
Advective Velocity = −380.0 m/hr
window width = 2.00 hours
20
15
10
5
0
ln(F/F₀)
−2000
0
2000
adjusted distance (m)
S−>N

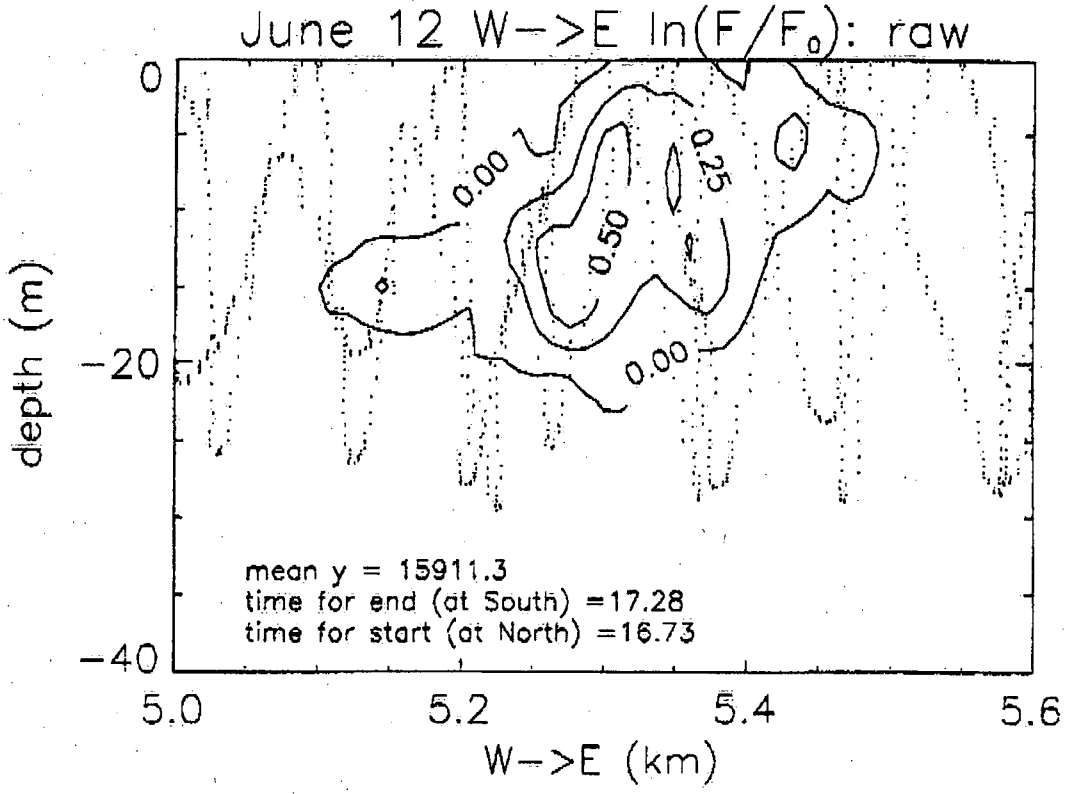
June 12 W->E ln(F/F0): raw
0
-20
-40
depth (m)
0.00
0.25
0.50
0.00
mean y = 15911.3
time for end (at South) =17.28
time for start (at North) =16.73
5.0
5.2
5.4
5.6
W->E (km)

Canada Centre for Inland Waters
P.O. Box 5050
867 Lakeshore Road
Burlington, Ontario
L7R 4A6 Canada

National Hydrology Research Centre
11 Innovation Boulevard
Saskatoon, Saskatchewan
S7N 3H5 Canada

St. Lawrence Centre
105 McGill Street
Montreal, Quebec
H2Y 2E7 Canada

Place Vincent Massey
351 St. Joseph Boulevard
Gatineau, Quebec
K1A 0H3 Canada

Centre canadien des eaux intérieures
Case postale 5050
867, chemin Lakeshore
Burlington (Ontario)
L7R 4A6 Canada

Centre national de recherche en hydrologie
11, boul. Innovation
Saskatoon (Saskatchewan)
S7N 3H5 Canada

Centre Saint-Laurent
105, rue McGill
Montréal (Québec)
H2Y 2E7 Canada

Place Vincent-Massey
351 boul. St-Joseph
Gatineau (Québec)
K1A 0H3 Canada